RSC Advances

ROYAL SOCIETY OF CHEMISTRY

www.rsc.org/advances

RSC Advances

RSCPublishing

ARTICLE

Rigid Jeffamine-included polyrotaxane as hydrogen-bond template for salicylideneazine with aggregation-enhanced emission

Cite this: DOI: 10.1039/xoxxoooooox

Received ooth January 2012,
Accepted ooth January 2012

DOI: 10.1039/xoxxoooooox

www.rsc.org/

Po-Chiao Huang, Li-Yang Lin, Deng-Jie Yang, and Jin-Long Hong*

Because restricted molecular rotation is the main mechanism responsible for the aggregation-induced emission (AIE), a Jeffamine-included polyrotaxane (JCD) was therefore used in this study as rigid template to impose effective rotational restriction on the AIE-active luminogen of 1,2-bis(2,4-dihydroxybenzylidene)hydrazine (CN4OH). Besides rigidifying the flexible Jeffamine chain, the β–cyclodextrin (β-CD) rings of JCD also provided hydroxyl (OH) groups to hydrogen bond to the OHs of CN4OH, furnishing emissive CN4OH/JCD(x/y) (x/y: molar ratio between CN4OH and JCD) blends with emission efficiency higher than the pure CN4OH itself. Dependent on the composition of the blends, CN4OHs in the blends are arrayed differently to experience varied levels of rotational restriction and thus emit with an intensity correlated with molecular arrangement of the CN4OHs in the blends. The relationship between molecular arrangement, restricted molecular rotation and AIE-oriented emission behavior is the focus of this study.

Introduction

Discovery of non-conventional luminogens with aggregation-induced emission (AIE)[1,2] property has drawn lots of research interests[3-9] regarding the beneficial emissive behaviour in the aggregated state. Aggregation is considered to be detrimental to emission for the traditional organic luminognes with planar geometry but for AIE-active luminogens (AIEgens), aggregates formed in the solution and solid states nevertheless emit with higher intensity than the dilute solution state. With the beneficial strong emission of the aggregates, AIEgens constructed from different structural units, such as tetraphenylethylene,[10,11] phenothiazine,[12,13] anthracene,[14,15] triphenylethylene,[16.17] distyrylanthracene,[18,19] carbazolyl[20,21] groups, AIE-active metal complexes[22,23] and polymers[24-26], had been prepared and characterized. Theoretical study concluded that the restriction of intramolecular rotations and vibrations (RIR and RIV)[9,27,28] are the main causes for the AIE phenomena observed in the propeller-shaped and shell-like AIEgens, respectively. Essentially, RIR is the main mechanism responsible for the AIE phenomenon since most of the AIEgens discovered nowadays are propeller-shaped molecules. By efficient RIR in the aggregated state, the non-radiative decay pathways of the exciton via vibrational/torsional energy relaxation can be largely reduced, resulting in the desired enhanced emission.

Inherent bulky substituent is no doubt effective in reinforcing RIR for the propeller-shaped AIEgens. However, external physical constraints also provide abundant resources for the deposition of rotational restriction on the AIEgens. Intuitively, rigid template is an ideal cornerstone for furnishing firm grips on AIEgens through favourable specific interactions, such as hydrogen bond (H bond)[29] between the AIEgen and the rigid template. Several H-bonded AIEgen/template blend systems[30-33] were therefore prepared in our laboratory. With effective H bond interactions to impose rotational restriction, AIEgens in the blends always emitted with higher emission intensity than pure AIEgens itself. The result clearly indicated that the key factor controlling the emission intensity is the

effective rotational restriction rather than the amounts of the luminescent AIEgens in the blends.

Salicylideneazine[34 –38] derivatives possess a six-membered, *pseudo* enolimine ring maintained by intramolecular H bond interaction between the hydroxyl (OH) group and the imine (C=N) nitrogen atom. For unbridged imine dyes, the C=N isomerization in the excited state is considered to be the predominant decay pathway but for enolimines with bridged C=N bonds (e.g. CN4OH in Scheme 1) an excited-state intramolecular proton transfer (ESIPT)[39 – 46] process is responsible for its radiative emission behaviour. Upon photoexcitation, fast transfer of the OH protons to C=N nitrogen quickly converts the excited enol (E*) into the excited keto (K*), giving rise to emission band with a large Stoke shift. In solution, CN4OH[36,47] emits weakly due to the twisted ketonic excited state whereas in the aggregated state, a planar dimer with the aromatic rings effectively locked by the intramolecular H bonds emits intensely. The OHs of CN4OH can be conveniently H-bond to pyridine rings of poly(vinyl pyridine) (PVP)[48]. Initially, preferable H-bonding between *p*-OHs of CN4OH and pyridine rings of PVP occurs to result in strong emissive CN4OH/PVP blends. However, when more PVPs are loaded in the blends, excess pyridine rings start to H-bond to the *o*-OHs of CN4OH and rupture the enolimine rings to result in the reduced emission of the blends.

With the hollow truncated cone, cyclodextrin molecules (CDs) can be used as host materials for including small molecules[49-51] or linear polymers[52-58], generating different polypseudorotaxane or polyrotaxane applied in controlled release of drugs in living organisms[59-61]. The hydrophobic cavity of CDs is also an ideal site for imposing efficient RIR required for AIE activity. A diboric acid tetraphenylethene (TPE) derivative[62] can cooperatively bind to two pairs of alternative diols on a β-CD, resulting in highly-emissive solution due to the effective RIR of the CD-incorporated TPE derivative. Alternatively, TPE was linked to the α-, β- and γ-CDs[63] through ester bonds. Solution emission of the β-CD-linked complex is weaker than α-CD-incorporated complex but is stronger than the one linked by γ-CD. The highest emission efficiency of the α-CD-linked complex is owing to that the smaller cavity of α-CD restricts the motions of luminogen more efficiently than the larger-sized β- and γ-CD cavities. More recently, amphiphilic AIEgens containing TPE moiety[64] were prepared and reacted with γ-CD to show new insight for AIE behaviour. When included in the cavity of γ-CD, the amphiphilic AIEgens showed an enhanced monomer emission and a decreased aggregate emission. Recently, Jeffamine-included β-CD (JCD) with cationic ammonium terminals[65] was used as a rigid template to complex with the sulfonate anions of a tetraphenylthiophene derivative (TPS), resulting in an ionic complex, which emitted with superior emission intensity than complex from TPS and the flexible Jeffamine. The role of rigid template in imposing effective RIR on AIEgen was demonstrated in this study. All above examples illustrate the use of CDs in constructing new AIE-active systems.

In this study, a Jeffamine-included β-CD (JCD, Scheme 1) is used as rigid template to mix with different amounts of CN4OHs, resulting in AIE-active CN4OH/JCD(x/y) (x/y: molar ratio between CN4OH and JCD) blends of varied emission efficiencies due to different levels of rotational restriction imposed on the CN4OHs. The β-CD rings of JCD serve as rigid component to stiff the flexible Jeffamine (amino-terminated poly(propylene glycol)) chain, resulting in rigid template for imposing effective rotational restriction on the incorporated AIEgens. Besides as rigid component, the β-CD rings of JCD also provide OH groups for H bonding to the implanted AIEgens of CN4OHs. Through favourable H-bond interactions between different amounts of JCD and CN4OH, all solid blends of CN4OH/JCD(x/y) are emitters with emission intensity higher than pure CN4OH itself. The study also suggests that the emission efficiency of the blends does not follow a monotonous dependence on the content of AIEgen but rather it correlates with molecular arrangements of the CN4OHs in the blends. As correlated to our previous study on the CN4OH/PVP blends[48], the molecular arrangements of CN4OHs are related to their binding fashions to the β-CD rings of JCD (Scheme 1). When the H-bonding is between the *p*-OHs of CN4OH and β-CD ring (route i), parallel arrays of CN4OHs result in crystalline structure, within which AIEs are firmly fastened by the tightly-packed crystalline lattice and therefore emit intensely due to the effective rotational restriction. In contrast, if H-bonding takes place on the *o*-OHs of CN4OHs and β-CD (route ii), the emission intensity of the blends will be largely reduced because the lateral binding fails in forming parallel, crystalline packing of CN4OHs. When the *o*-OHs of CN4OH was H bonded by JCD, the *pseudo* six-membered enolimine ring was also ruptured and the liberated C=N bond will be free to isomerize in the excited state, resulting in emission quenching. Factors of controlling molecular arrangement of CN4OHs in the blends thus determine the rotational

restriction and the emission efficiency of the AIE-active blends. The interrelationship between molecular arrangement, restricted molecular rotation and the AIE-related emission behaviour will be discussed following the manuscript.

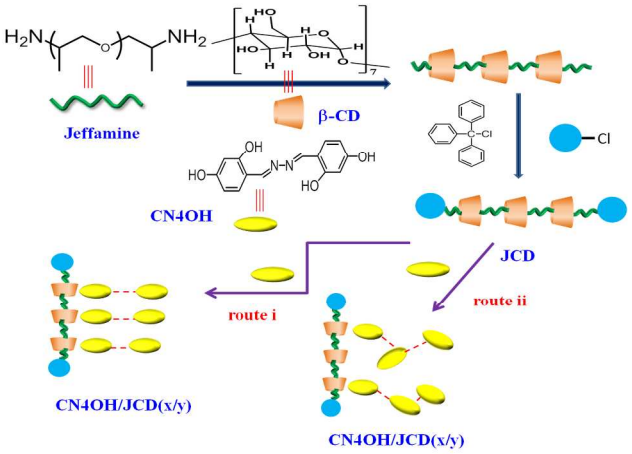

Scheme 1 Synthesis of JCD and its complexation with CN4OHs to prepare CN4OH/JCD(x/y) blends and the possible H bonding fashions involved in the blends.

Experimentals

Materials

Jeffamine D-400 (diamino-terminated poly(propylene glycol), Alfa Assar) and β-cyclodextrin (TCI, 95%) were used directly. CN4OH [48] and JCD[66] were synthesized according to the published procedures. Preparation of JCD was detailed below:

Preparation of Jeffamine-included -CD (JCD).

Solution of β-CD (0.38 g, 0.335 mmol) in deionized water (15 mL) was added into the stirred solution of Jeffamine D400 (2.92 g) in deionized water (4 mL). The whole solution was then under ultrasonic agitation for overnight. The white precipitant in the solution mixtures was then collected by filtration and was dried in the vacuum oven at 60 °C for 24 h. The resulting complex was then mixed with chorotriphenylmethane (4.52 g) in DMF (30 mL) in prior to the addition of triethylamine (2 mL). The reaction mixtures were subjected to vigorous stirring at room temperature for 24 h. The reaction product was then precipitated from diethyl ether and dried in vacuum oven at 60°C for 24 h. ^{1}H NMR (500 MHz, D_2O) (ppm): 7.32 (d, 12H, aromatic H), 7.34 (d, 12H, aromatic H), 7.19 (d, 6H, aromatic H), 5.75 (br, 14H overlapped), 4.8 (d, 7H), 4.45 (m, 6H), 3.64 (br, 28H overlapped), 3.08(br, 14H overlapped), 1.16(d, 3H, CH_3) (Figure S1).

Preparation of CN4OH/JCD blends

The calculated amounts of CN4OH and JCD were dissolved in THF and the whole mixtures were stirred vigorously at room temperature for 24 h. The resulting complex solution was then subjected to rotary evaporation to remove THF. The final product was obtained by drying in vacuum oven at 60 °C for 24 h.

Instrumentations

The ^{1}H NMR spectra were recorded by a Varian Unity Inova-500 MHz. UV-vis absorption spectra were obtained from an Ocean Optics DT 1000 CE 376 spectrophotometer. PL emission spectra were recorded by a LabGuide X350 fluorescence spectrophotometer using a 450 W Xe lamp as the continuous light source. Quantum yields (Φ_F) of the solutions were determined by using a quinine sulfate as a standard solution and integrating sphere was used for the solid sample. The wide-angle X-ray diffraction (WAXD) spectra were obtained from a Siemens D5000 diffractometer. Thermal transition of the blends was determined from a TA Q-20 differential scanning calorimeter (DSC) calorimeter with a scan rate of 10 ^{o}C/min under nitrogen. Particle sizes in selective solvent pairs were measured by dynamic light scattering instrument (DLS) on a Brookhaven 90 plus spectrometer at room temperature. An argon ion laser operating at 658 nm was used as light source.

Results and discussion

According to Scheme 1, the rigid JCD template was primarily prepared from a two-step synthesis route. First, β-CD was ultrasonically shaken with Jeffamine to result in Jeffamine-included β-CD, which was then capped by chlorotriphenylmethane to obtain the desired JCD. The ^{1}H NMR spectrum (Figure S1) of JCD revealed an average of 3.1 β-CD rings per Jeffamine chain according to the integrated ratio between propylene methyl protons (proton **a**) of Jeffamine and acetal carbon proton (proton **b**) of β-CD. JCD was then mixed with different amounts of CN4OHs, resulting in solid CN4OH/JCD(x/y) (x/y: molar ratio between CN4OH and JCD) blends with low (x/y < 1) and high (x/y >1) contents of CN4OHs for study.

Before discussion on the solid samples, we needed to identify the function of JCD as effective template for CN4OH; for this, characterization on the solution mixtures of CN4OH/JCD(x/y) was primarily conducted.

Solution mixtures of CN4OH/JCD(x/y)

Solution mixtures of CN4OH/JCD(x/y) containing excess JCD (x/y < 1) were used here to prove that JCD is an effective template in imposing rotational restriction on CN4OH. With excess JCDs, CN4OHs in the solutions are considered to be bound by JCDs and will emit with an intensity dependent on how well they are securely locked by the rigid JCDs. Preferable H bond interaction between CN4OH and JCD should already take place in the solution state since solution mixtures of CN4OH/JCD(x/y) exhibit a composition-dependent emission behaviour (Figure 1). All the solution mixtures investigated in Figure 1 contain constant amounts of CN4OH (= 10^{-3} M); therefore, the emission difference observed in Figure 1 should be attributed to the amounts of JCDs added in the solutions. Solution of pure CN4OH emitted dimly but the inclusion of JCD caused a large emission enhancement. Under the premise that all solutions contain the same amounts of CN4OHs, the solution emission intensity nevertheless increases with increasing JCD content from an x/y = 1/3 to 1/12. The emission enhancement observed here is therefore related to the amounts of CN4OHs anchored by JCDs in the solutions. By H bonding to the OH groups of rigid JCDs, the anchored CN4OHs are clumsy in rotational motion, thus emitting efficiently with the operative AIE activity. More JCDs added in the solutions generate more of the anchored CN4OHs, which contributes to the emission enhancement of the solution mixtures.

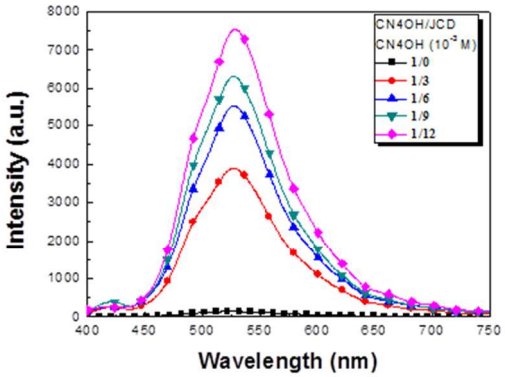

Fig. 1 Solution emission spectra of CN4OH/JCD(x/y) mixtures with a constant concentration of CN4OH (= 10^{-3}M) in DMSO. (λ_{ex} = 365 nm)

The ^{1}H NNR spectrometer is a powerful tool for evaluating the extent of rotational restriction in the solution state. It was suggested[27,67] that the fast conformational exchanges caused by the fast intramolecular rotation give sharp resonance peaks, whereas the slow exchanges due to the slow rotations broaden the resonance peals. The ^{1}H NMR analysis was then extended to polymer[68] and polymer blend[33] systems and the results suggested that the rotational restrictions in the blend systems are so effective that the corresponding resonance bands became reduced in intensity or disappeared due to the insufficient power of the magnetic field in igniting the molecular motion of the frozen bonds. We therefore applied ^{1}H NMR analysis on the present system but for the sake of eliminating the potential complication from concentration difference, the ^{1}H NMR analysis in Figure 2 was performed using solutions with the same amounts of CN4OHs (= 10^{-3} M). Spectrum of pure CN4OH contains three sets of large resonance peaks in correlation to the aromatic protons **a**, **b** and **c**, respectively Addition of JCDs in the solutions resulted in the upfield shift and the large reduction of the resonance peaks in the spectra of CN4OH/JCD(1/3), (1/9) and (1/12). Increasing amounts of JCDs in the solutions generated more anchored CN4OHs, which are firmly held by the rigid JCD and are therefore clumsy in response to the ignition of the external magnetic field. The ^{1}H NMR analysis thus demonstrated that JCD is indeed an effective template in imposing the required rotational restriction on CN4OH.

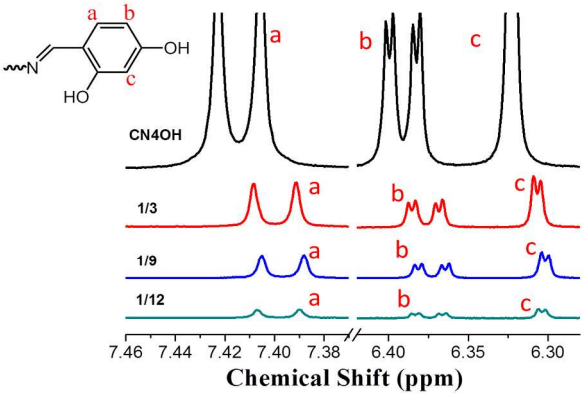

Fig. 2 ^{1}H NMR spectra of pure CN4OH and the CN4OH/JCD(x/y) mixtures with a constant amounts of CN4OH (10^{-3} M) in d_6-DMSO.

Solid CN4OH/JCD(x/y) blends

Solid blends containing low (x/y < 1) and high (x/y > 1) fractions of CN4OH were prepared and their emission spectra were

compared with pure CN4OH in Figure 3A and B, respectively. Consistent with our previous blend systems[30-33], the CN4OH/JCD (x/y) blends all emitted with higher intensity than pure CN4OH. For the blends with fewer (x/y < 1) CN4OHs, the resolved emission intensity (Figure 3A) was increased upon increasing JCD content from the blends of CN4OH/JCD(1/3) to (1/12). Quantum yield (Φ_F, Table 1) measured from integration sphere also follows the same result that increasing JCD content from CN4OH/JCD(1/3) to (1/12) raised the Φ_F values from 17 to 28%. The blend containing less CN4OHs (e.g. CN4OH/JCD(1/12)) is superior in emission efficiency than the blend with more luminogens (e.g. CN4OH/JCD(1/3)). Therefore, it is the rotational restriction, rather than the amounts of AIEgens, that controls the final emission efficiency of the AIE-active blends.

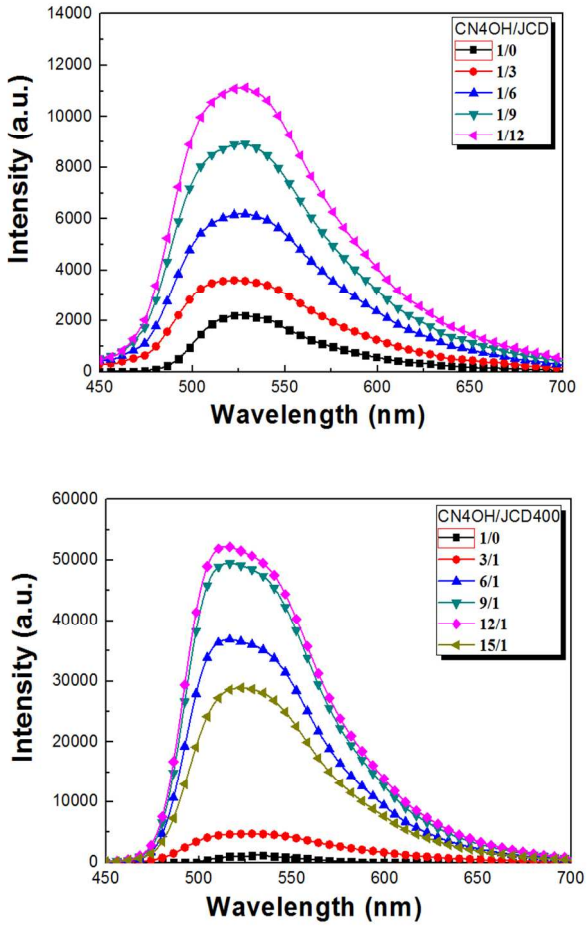

Fig. 3 Solid emission spectra of CN4OH/JCD(x/y) with (A) x/y < 1 and (B) x/y > 1. (λ_{ex} = 365 nm)

Increasing the content of AIEgen decreases the emission efficiency for the blends containing fewer (x/y < 1) CN4OHs but such a trend is not followed in the blends containing large amounts (x/y >1) of CN4OHs. Initially, the resolved emission intensity (Figure 3B) of the blends was increased upon with increasing CN4OH content from the blends of CN4OH/JCD(3/1) to (12/1) but further loading of CN4OHs nevertheless resulted in the significant intensity reduction in the spectrum of CN4OH/JCD(15/1). This result reflects subtle change of the molecular arrangement of the AIEgens in the blends and will be discussed next. The observed variations of the emission intensity are in line with the resolved Φ_{Fs} summarized in Table 1. CN4OH/JCD(3/1) emits with a higher Φ_F than pure CN4OH (18 vs 15 %) and increasing CN4OH content eventually raises the Φ_F to the highest value of 78% for the blend of CN4OH/JCD(12/1). However, raising content of CN4OHs resulted in the lowering of Φ_F to a value of 37% for CN4OH/JCD(15/1). From the blends of CN4OH/JCD(12/1) to (15/1), molecular arrangement of the luminescent CN4OHs must be under major transformation to result in such a large change on the emission efficiency..

WAXD spectra of the solid blend

The WAXD spectra of Fig 4A and 4B provide information regarding the crystalline structures of the blends with low (x/y < 1) and high CN4OH (x/y > 1) contents, respectively. Pure JCD and CN4OH are semi-crystalline material with the clearly-visible crystalline diffraction peaks (Figure 4A) over the broad amorphous background. For the blends containing fewer (x/y < 1) CN4OHs (Figure 4A), the incorporation of CN4OHs tends to interrupt the crystalline structure of JCDs. Initially, certain fractions of crystalline JCDs are still present in the blends of CN4OH/JCD(1/12); however, further incorporation of CN4OHs in the blends of CN4OH/JCD(1/9), (1/6) and (1/3) resulted in new structures with broad diffraction peaks in the range from 2θ = 12 to 18°. The sharp diffraction peaks of pure CN4OH are all absent in the spectra of the corresponding blends; therefore, the minor CN4OHs are considered to be completely dispersed by JCDs. Crystallinity calculated from the WAXD spectra was summarized in Table 1 and the results indicate that the blend's crystallinity slightly increases upon increasing JCD content in the blends. Favourable H bond interactions between JCD and CN4OH must be prevail in the blend and act to rupture the crystalline arrays of CN4OHs. Blends with higher crystallinity also emit with higher efficiency, which is reasonable considering crystals

with less voids and free volumes are efficient in restricting the rotational motion of the AIEgens inside the crystalline lattices. This result is correlated with crystallization-enhanced emission (CEE) behaviour observed in several AIEgena[69-74]. For example, the AIE-active triphenylethylene derivative[48] emitted with lower intensity when it was transformed from crystalline to amorphous states by increasing the nonsolvent water fraction of the DMF/water mixtures.

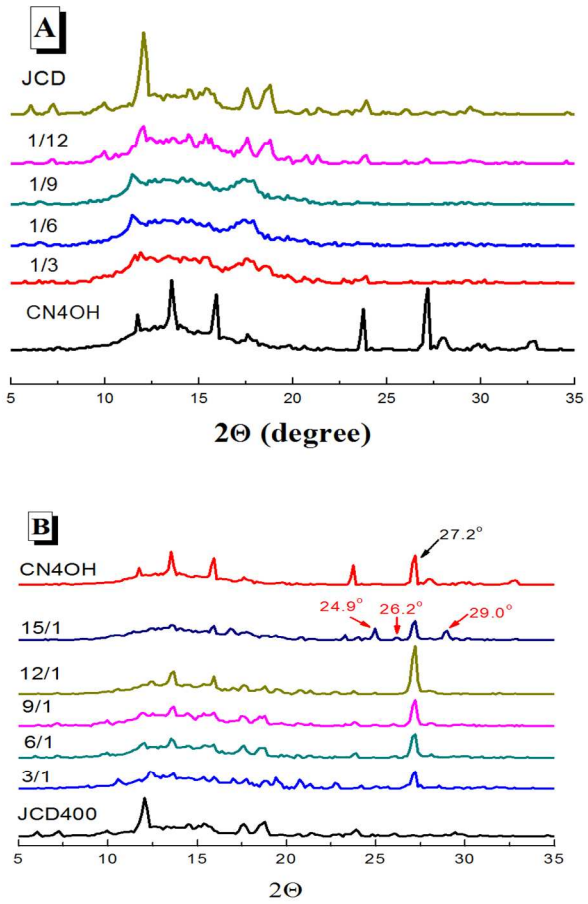

Fig. 4 WAXD spectra of CN4OH/JCD(x/y) blends with (A) x/y < 1 and (B) x/y > 1.

As illustrated in Figure 4B, spectra of blends with excess (x/y >1) CN4OHs contain the characteristic diffraction peaks of crystalline CN4OHs. We may assess the molecular packing of CN4OHs by the main diffraction peak at 2θ = 27.2° (indicated by black arrow) that it gradually becomes larger in intensity (compared to the amorphous background) when more CN4OHs are incorporated in the blends from CN4OH/JCD(3/1) to (12/1). Crystalline structures beneficial for imposing effective rotational restriction are thus developed upon increasing the content of CN4OH; nevertheless, the advantageous role of CN4OHs is not always hold since a reduced intensity for the peak at 2θ = 27.2° was resolved in spectrum of CN4OH/JCD(15/1). Careful inspection also revealed that the spectrum of CN4OH/JCD(15/1) contains few new diffraction peaks at 2θ = 24.9, 26.2, 29.0° (indicated by red arrows), which indicates certain fractions of CN4OHs in the blend of CN4OH/JCD(15/1) were arrayed in a pattern different from the CN4OHs in other blends. The calculated crystallinity (Table1) is consistent with the WAXD spectra that crystallinity increased in blends from CN4OH/JCD(3/1) to (12/1) but decreased in the blend of CN4OH/JCD(15/1). Blends with higher crystallinity also emit with higher efficiency; therefore, the resolved Φ_Fs increases from 18 to 78% as the crystallinity increases from 38 to 71% from the blends of CN4OH/JCD(3/1) to (12/1) but the reduced crystallinity of 57 % results in the lower Φ_F of 37% for CN4OH/JCD(15/1).

Table 1 Quantum yield (Φ_F) and crystallinity of CN4OH/JCD(x/y) blends.

A. CN4OH/JCD(x/y) with x/y <1						
x/y	0/1	1/3	1/6	1/9	1/12	
wt% of CN4OH(%)	0	2.02	1.01	0.681	0.512	
Φ_F (%)[a]	-	17	22	25	28	
Crystallinity (%)[b]	73	42	46	47	52	
B. CN4OH/JCD(x/y) with x/y >1						
x/y	1/0	3/1	6/1	9/1	12/1	15/1
wt% of CN4OH(%)	100	15.62	27.03	35.71	42.55	48.08
Φ_F (%)[a]	15	18	56	75	78	37
Crystallinity (%)[b]	38	40	64	69	71	57

[a] determined from integration sphere.

[b] calculated from the WAXD spectrum.

Thermal analysis of the solid blends

DSC traces of the CN4OH/JCD(x/y) blends with x/y < 1 and > 1 are given in Figure 5A and 6A, respectively, to provide

information regarding possible molecular arrangements of the blends.

As illustrated in Figure 5A, the broad melting transition of pure JCD may be attributed to the large JCD aggregates of varied particle sizes. Through interchain H bond interactions between the OHs of the JCD chains, formation of large JCD aggregates of varied sizes is highly probable. For the blends containing more JCDs, the minor CN4OHs implanted in the blends do not largely alter the JCD aggregates formed since DSC traces of the blends resulted in broad melting transition in the same temperature ranges. More conclusive support can be illustrated by the melting enthalpy (ΔH, Figure 5B), involved in the melting transition, that it increased in linear proportional to the molar fraction of JCDs in the blends. Therefore, melting involved in the blends of low CN4OH content mainly concerns the large JCD aggregates.

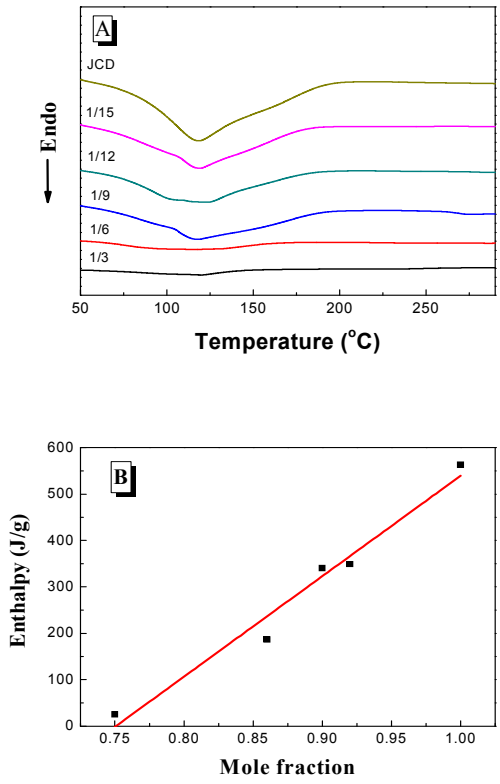

Figure 5 (A) DSC thermogram of CN4OH/JCD(x/y) with x/y < 1 (heating rate = 10 °C/min) and (B) the low-temperature melting enthalpy versus molar fraction of JCD in the blend.

Molecules in the blends containing excess CN4OHs (x/y > 1) are considered to have different packing manner from those in the blends of low CN4OH content considering there are extra high-temperature thermal transitions in the DSC traces (Figure 6A) of for the blends. The low- and high-temperature thermal transitions are attributed to the molecular motions involved in the JCD- and CN4OH-rich phases, respectively. Compared to the broad melting transition observed in Figure 5A, the low-temperature melting endotherms observed here are higher in temperatures and sharper in shape. It is then envisaged that the low-temperature melting in the blends of high CN4OH content should involve the CN4OH-anchored JCD particles. That the low-melting transition gradually shifted to lower temperatures with increasing CN4OHs should correlate with the fact that the implanted CN4OHs in the CN4OH-rich phase were already anchored by JCDs. The lowering of the melting transition from CN4OH/JCD(3/1) to (15/1) is due to the size reduction of the JCD aggregates. By H bonding to JCDs, the small-mass CN4OHs chopped the large JCD aggregates into smaller ones with lower melting temperatures.

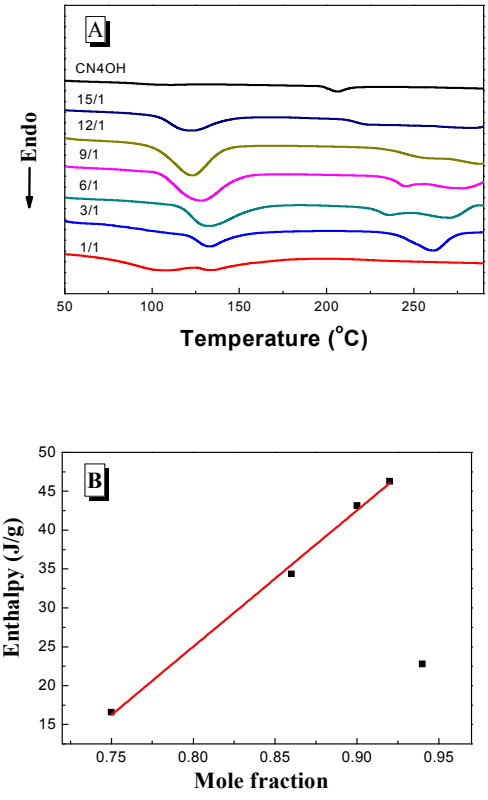

Figure 6 (A) DSC thermogram of CN4OH/JCD(x/y) with x/y > 1 (heating rate = 10 °C/min) and (B) the low-temperature melting enthalpy versus molar fraction of CN4OH in the blends.

The enthalpy (ΔH) adopted from the low-temperature melting transition are associated with the molar fraction of CN4OH in the blends (Figure 6B). Initially, ΔH is linearly proportional to the molar fraction of CN4OHs in the blends from CN4OH/JCD(3/1) to (12/1). However, further implantation of CN4OHs in the blend of CN4OH/JCD(15/1) lowered the ΔH significantly. The low ΔH indicates the presence of disordered, anchored CN4OHs in the JCD-rich phase of CN4OH/JCD(15/1). The low ΔH observed for CN4OH/JCD(15/1) is in line with the low crystallinity evaluated from WAXD and is also correlated with the high-temperature thermal transition discussed next.

The high temperature thermal transition reflects the subtle phase behaviour of the CN4OH-rich phase. For CN4OH/JCD(3/1), the high-temperature melting endotherm occurred at temperatures higher than the pure CN4OH. Extra CN4OH molecules in the blend are supposed to follow the parallel packing of the pre-existing, anchored CN4OHs (route i, Scheme 1), resulting in tightly-packed crystalline arrays with high melting temperature. Further loading of CN4OHs resulted in complicated thermal behaviour regarding the multiple melting-recrystallization process shown in the DSC traces of CN4OH/JCD(6/1), (9/1) and (12/1). The cause responsible for the multiple thermal transitions is hard to identify presently but fortunately, DSC trance of CN4OH/JCD(15/1) is simple and contains only one single glass transition in the high-temperature region. Certain CN4OHs in CN4OH/JUCD(15/1) are therefore randomly packed to result in the glass transition. In addition, the high-temperature glass transition is considered to be associated with the low enthalpy involved in the low-temperature melting process. Through intermolecular H bond interactions, CN4OHs in the CN4OH-rich phase should be associated with packing manner of the anchored CN4OHs in the JCD-rich phase. More crystalline JCD aggregates favor the formation of well-packed CN4OHs in the CN4OH-rich phase whereas misaligned, anchored CN4OHs in the JCD-rich phase result in the amorphous CN4OH-rich phase. Anchored CN4OHs in the blends of CN4OH/JCD(3/1), (6/1). (9/1) and (12/1) are packed regularly to result in crystalline CN4OHs in the CN4OH-rich phase but for CN4OH/JCD(15/1) the disordered, anchored CN4OHs generated certain amorphous CN4OH-rich phase besides the regular crystalline lattices.

Molecular arrangement of the solid blends

As illustrated in Scheme 1, different H bond packing manners involved in CN4OH/JCD(x/y) blends resulted in CN4OHs of varied molecular arrangements, which in turn determine the emission efficiency of the blends. In blends containing excess JCDs (x/y < 1), the minor CN4OHs are anchored and immobilized by the rigid JCDs but in blends containing less amounts of JCD (x/y >1), majority of CN4OHs form separate CN4OH-rich phase with the molecular arrangement strongly associated with the packing manner of the anchored CN4OH in the pre-existing JCD-rich phase. Particularly, molecular arrangement of the highly CN4OH-loaded CN4OH/JCD(15/1) is different from others and hence, needed to be considered separately. Accordingly, we classified possible molecular arrangements of the solid CN4OH/JCD(x/y) blends into situations of x/y < 1, x/y > 1 and x/y = 15/1 (Scheme 2).

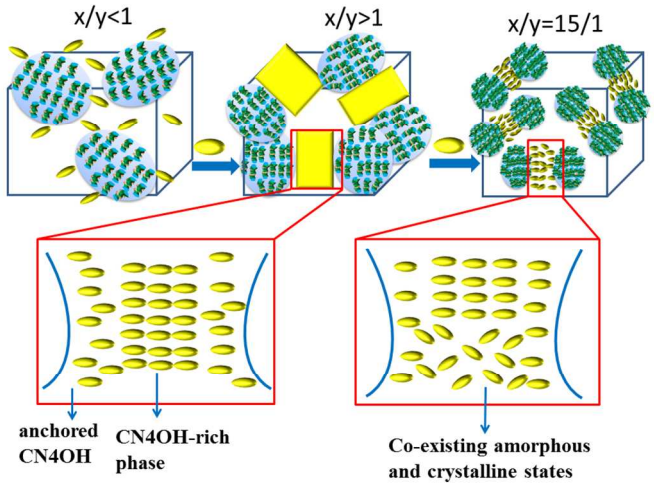

Scheme 2 Transformation of molecular arrangements upon increasing CN4OHs in the blends.

Large JCD aggregates are the fundamental units existing in the blends containing fewer CN4OHs (x/y <1). For pure JCD, self-association of JCDs can be easily achieved through interchain H bond interactions between the inherent OH groups, resulting in large aggregated JCD particles with broad size distribution. For blends containing fewer CN4OHs (x/y < 1), the minor CN4OHs were considerably H bonded and dispersed by the majority of JCDs. The large, crystalline JCD aggregates are the fundamental structure units remained relatively intact in the presence of minor CN4OHs. Because JCD aggregates are the main structures in blends containing fewer CN4OHs, the resolved ΔHs are linearly proportional to the molar fraction of the loaded JCDs (Figure 6B). Held by the rigid

JCD templates, the anchored CN4OHs are so immobile that they emit with intensity higher than pure CN4OH itself.

For blends containing excess CN4OHs (x/y > 1), the interrelating JCD- and CN4OH-rich phases are responsible for the low- and high-temperature thermal transitions (Figure 6A), respectively. The JCD-rich domains basically concern JCD aggregates and the anchored CN4OHs in the surface areas of the JCD aggregates. Initially, the anchored CN4OHs served as starting sites for further reaction with the implanted CN4OHs in the CN4OH-rich domains. Through favourable H bond interactions between the *p*-OHs of CN4OHs (route i in Scheme 1), the anchored CN4OHs directed the following CN4OHs to pack in aligned and parallel fashion, thereby generating highly-emissive, crystalline CN4OHs due to effective rotational restriction in the tightly-packed crystalline lattice. In contrast, H bond interactions to the lateral *o*-OHs of the anchored-CN4OHs (route ii in Scheme 1) resulted in misaligned, amorphous CN4OHs. Through intermolecular H bond interactions, molecular arrangement of the anchored CN4OHs is considered to couple with the molecular packing of the excess CN4OHs in the CN4OH-rich phase. Anchored CN4OHs in preferable crystalline packing lead to crystalline CN4OHs in the CN4OH-rich phase whereas misaligned, anchored CN4OHs result in amorphous CN4OH-rich phase.

By favourable intermolecular H bond interactions, large JCD aggregates were dissociated and chopped by CN4OHs into smaller aggregates with lower melting transitions. Smaller JCD aggregates possess larger surface areas for accepting more CN4OHs but the small particles also limited inter-aggregates spaces leaving for the accommodation of implanted CN4OHs. For the blends from CN4OH/JCD(3/1) to (12/1), loading CN4OHs in the blends resulted in the proportional increase of the low-temperature ΔH, which refers to the continuous growth of the tightly-packed, anchored CN4OHs. The crystalline anchored CN4OHs also led to crystalline CN4OHs in the CN4OH-rich phase. Because the molecular motions are securely locked in the crystals, corresponding blends therefore emitted intensely. For CN4OH/JCD(15/1) with the highest content of CN4OH, there are limited inter-aggregates space available for the large amounts of CN4OHs. Therefore, excess CN4OHs were forced to penetrate into the free spaces between β-CDs of JCD and started to bond to the lateral *o*-OHs of the anchored CN4OHs, resulting in misaligned CN4OHs responsible for the new diffraction peaks observed in WAXD spectrum (Figure 3B) and the lowering of the low-temperature ΔH. The misaligned CN4OHs in the JCD-rich phase are also responsible for the disordered CN4OHs in the CN4OH-rich phase. Besides the crystalline, parallel CN4OHs with the H-bonded *p*-OHs, the CN4OH-rch phase of CN4OH/JCD(15/1) also contains the misaligned, amorphous CN4OHs formed through lateral H-bond interactions. All the disordered CN4OHs in the blend of CN4OH/JCD(15/1) are responsible for its lower Φ_F compared to other blends with higher crystallinity (i.e. CN4OH/JCD(6/1), (9/1) and (12/1)), considering the inefficient rotational restriction in the loosely-packed amorphous regions.

The results suggested that JCD served as efficient rigid template in reinforcing rotational restriction of CN4OH if appropriate amounts of CN4OHs were applied in the blends. With fewer CN4OHs (x/y <1), most of the CN4OHs were securely held by JCDs and emitted efficiently with the operative rotational restriction. With more CN4OHs (x/y > 1), well-packed CN4OHs in the JCD- and CN4OH-rich phases led to crystalline blends with the inherent CN4OHs firmly held in the crystalline lattices. The corresponding blends are therefore strong emitters with the operative rotational restriction in the crystalline blends. With the limited inter-aggregates spaces, the highly CN4OH-loaded CN4OH/JCD(15/1) contains certain misaligned, amorphous CN4OHs and its emission efficiency is comparably lower than the CN4OH/JCD(6/1). (9/1) and (12/1). Molecular arrangement of CN4OHs are therefore the decisive factor controlling the emission efficiency of the CN4OH/JCD(x/y) blends.

Conclusion

A Jeffamine-included polyrotaxane (JCD) was prepared and served as rigid template to H bond to different amounts of CN4OH, resulting in CN4OH/JCD(x/y) blends with solid emission intensity dependent on the amounts of CN4OH loaded in the blends.

Solution emission behaviour clearly demonstrates the role of JCD in imposing effective rotational restriction on CN4OHs. Solution emission of the CN4OH/JCD mixtures was increased with increasing JCDs in the solutions. Increasing JCD content of the CN4OH/JCD mixtures also reduced the aromatic resonance peaks of the ^{1}H NMR spectra due to the increasing rotational restriction on CN4OHs. Therefore, JCDs are rigid templates effective in imposing rotational restriction on CN4OHs.

Emission efficiencies of the solid CN4OH/JCD(x/y) blends are all higher than pure CN4OH itself. It is then the rotational restriction, rather than the amounts of the AIEgens, controlling the final emission behaviour of the AIE-active blends. With fewer (x/y <1) CH4OHs, the emission efficiency of the blends was increased with increasing JCDs loaded in the blends. Though H bond interactions, the CN4OHs are firmly-held by the JCD aggregates and emit intensely due to the operative rotational restriction. For the blends containing excess (x/y > 1) CN4OHs, the emission efficiency was increased with increasing CN4OH content. The tightly-packed crystalline CN4OHs in both the JCD- and CN4OH-rich phases are responsible for the strong emission of the blends. Crystallinity of the blends is raised by the CN4OHs loaded in the blends and so is the emission efficiency of the blends. Nevertheless, further loading of CN4OHs result in the adverse emission reduction of the CN4OH/JCD(15/1) blend. Inside this highly-loaded blend, lateral binding to the *o*-OHs of CN4OH occurred to result in misaligned CN4OHs, which emit weakly due to the loose packing of the disordered CN4OHs. The correlation between molecular arrangement, rotational restriction and AIE-related emission behaviour are therefore illustrated in this study.

Acknowledgement

We appreciate the financial support from the Ministry of Science and Technology, Taiwan, under the contract no. NSC 102-2221-E-110-084-MY3.

Notes and references

Department of Materials and Optoelectronic Science, National Sun Yat-Sen University, Kaohsiung 80424, Taiwan, Republic of China. E-mail: jlhong@mail.nsysu.edu.tw; Tel: +886-7-5252000, ext 4065[*]

†Electronic Supplementary Information (ESI) available: [Fig S1–S2]. See DOI: 10.1039/b000000x/

1. J. Luo, Z. Xie, J. W. Y. Lam, L. Cheng, H. Chen, C. Qiu, H. S. Kwok, X. Zhan, Y. Liu, D. Zhu and B. Z. Tang, *Chem. Commun.*, 2001, 1740.
2. 2 B. Z. Tang, X. Zhan, G. Yu, P. P. S. Lee, Y. Liu and D. J. Zhu, *Mater. Chem.*, 2001, **11**, 2974.
3. 3 Y. Hong, J. W. Y. Lam and B. Z. Tang, *Chem. Commun.*, 2009, 4332.
4. 4 D. Ding, K. Li, B. Liu and B. Z. Tang, *Acc. Chem. Res.*, 2013, **46**, 2441.
5. 5 Z. Zhao, J. W. Y. Lam and B. Z. J. Tang, *J. Mater. Chem.*, 2012, **22**, 23726.
6. 6 M. Wang, G. Zhang, D. Zhang, D. Zhu and B. Z. J. Tang, *J. Mater. Chem.*, 2010, **20**, 1858..
7. 7 Z. Zhao, J. W. Y. Lam and B. Z. Tang, *Soft Matter*, 2013, **9**, 4564.
8. 8 Aggregation-Induced Emission: Fundamentals, ed. A. Qin, and B. Z. Tang, John Wiley & Sons, Ltd, NY, 2013.
9. J. Mei, Y. Hong, J. W. Y. Lam, A. Qin, Y. Tang and B. Z. Tang, *Adv. Mater.*, 2014, **26**, 5429.
10. X. Zhang, Z. Chi, H. Li, B. Xu, X. Li, S. Liu, Y. Zhanga and J. Xu, *J. Mater. Chem.*, 2011, **21**, 1788.
11. Z. Wang, J. H. Ye, J, Li, Y. Bai, W. Zhanga and W. He, *RSC Adv.*, 2015, **5**, 8912.
12. J. Zhang, B. Xu, J. Chen, L. Wang, and W. Tian, *J. Phys. Chem. C*, 2013, **117**, 23117.
13. S. Y. Su, H. H. Lin and C. C. Chang, *J. Mater. Chem.*, 2010, **20**, 8653.
14. B. Sun, X. Yang, L. Ma, C. Niu, F. Wang, N. Na, J. Wen and J. Ouyang, *Langmuir*, 2013, **29**, 1956.
15. X. Zhang, Z. Chi, B. Xu, C. Chen, X. Zhou, Y. Zhang, S. Liua and J. Xu, *J. Mater. Chem.*, 2012, **22**, 18505.
16. H. Li, Z. Chi, B. Xu, X. Zhang, Z. Yang, X. Li, S. Liu, Y. Zhanga and J. Xu, *J. Mater. Chem.*, 2010, **20**, 6103.
17. H. Li, Z. Chi, X. Zhang, B. Xu, S. Liu, Y. Zhang and J. Xu, *Chem. Commun.*, 2011, **47**, 11273.
18. J. He, B. Xu , F. Chen , H. Xia , K. Li , L. Ye and W. Tian, *J. Phys. Chem. C*, 2009, **113**, 9892.
19. B. Xu, J. Zhang, H. Fang, S. Ma, Q. Chen, H. Sun, C. Imc and W. Tian, *Polym. Chem.*, 2014, **5**, 479.
20. S. Dong , Z. Li and J. Qin, *J. Phys. Chem. B*, 2009, **113**, 434.
21. J. Huang, X. Yang, J. Wang, C. Zhong, L. Wang, J. Qina and Z. Li, *J. Mater. Chem.*, 2012, **22**, 2478.
22. Z. Wei, Z. Y. Gu, R. K. Arvapally, Y. P. Chen, R. N. McDougald, Jr., J. F. Ivy, A. A. Yakovenko, D. Feng, M. A. Omary, and H. C. Zhou, *J. Am. Chem. Soc.*, 2014, **136**, 8269.
23. N. B. Shustova, T. –C. Ong, A. F. Cozzolino, V. K. Michaelis, R. G. Griffin and M. Dincă, *J. Am. Chem. Soc.*, 2012, **134**, 15061.
24. X. Zhang, X. Zhang, L. Tao, Z. Chi, J. Xub and Y. Wei, *J. Mater. Chem. B*, 2014, **2**, 4398.
25. X. Zhang, X. Zhang, B. Yang, M. Liu, W. Liu, Y. Chena and Y. Wei, *Polym. Chem.*, 2014, **5**, 356.
26. M. C. Hsieh, C. H. Chien, C. C. Chang and T. C. Chang, *J. Mater. Chem. B*, 2013, **1**, 2350.
27. J. Chen, C. C. W. Law, J. W. Y. Lam, Y. Dong, S. M. F. Lo, I. D. Williams, D. Zhu and B. Z. Tang, *Chem. Mater.*, 2003, **15**, 1535.
28. J. Shi, N. Chang, C. Li, J. Mei, C. Deng, X. Luo, Z. Liu, Z. Bo, Y. Q. Dong and B. Z. Tang, *Chem. Commun.*, 2012, **48**, 10675.
29. S. H. Huang, Y. W. Chiang and J. L. Hong, *Polym. Chem.*, 2015, **6**, 497.
30. W. L. Chien, C. M. Yang, T. L. Chen, S. T. Li and J. L. Hong, *RSC Adv.*, 2013, **3**, 6930.
31. S. L. Deng, T. L. Chen, W. L. Chien and J. L. Hong, *J. Mater. Chem.*

C, 2014, **2**, 651.

32. K. Y. Shih, Y. C. Lin, T. S. Hsiao, S. L. Deng, S. W. Kuo and J. L. Hong, *Polym. Chem.*, 2014, **5**, 5765.
33. R. H. Chien, C. T. Lai and J. L. Hong, *J. Phys. Chem. C*, 2011, **115**, 20732.
34. T. Mutai, H. Tomoda, T. Ohkawa, Y. Yabe and J. Araki, *Angew. Chem., Int. Ed.*, 2008, **47**, 9522.
35. Y. Qian, S. Y. Li, G. Q. Zhang, Q. Wang, S. Q. Wang, H. J. Xu, C. Z. Li, Y. Li and G. Q. Yang, *J. Phys. Chem. B*, 2007, **111**, 5861.
36. W. X. Tang, Y. Xiang and A. J. Tong, *J. Org. Chem.*, 2009, **74**, 2163.
37. S. Scheiner and V. M. Kolb, *Proc. Natl. Acad. Sci. U. S. A.*, 1980, **77**, 5602.
38. H. Birkedal and P. Pattison, *Acta Crystallogr., Sect. C: Cryst. Struct. Commun.*, 2006, **62**, 139.
39. M. Y. Berezin and S. Achilefu, *Chem. Rev.*, 2010, **110**, 2641.
40. C. C. Hsieh, Y. M. Cheng, C. J. Hsu, K. Y. Chen and P. T. Chou, *J. Phys. Chem. A*, 2008, **112**, 8323.
41. M. M. Henary and C. J. Fahrni, *J. Phys. Chem. A*, 2002, **106**, 5210.
42. A. Mordzinski and A. Grabowska, *Chem. Phys. Lett.*, 1982, **90**, 122.
43. A. Douhal, F. Lahmani and A. H. Zewail, *Chem. Phys.*, 1996, **207**, 477.
44. S. Lochbrunner, T. Schultz, M. Schmitt, J. P. Shaffer, M. Z. Zgierski and A. Stolow, *J. Chem. Phys.*, 2001, **114**, 2519.
45. J. Goodman and L. E. Brus, *J. Am. Chem. Soc.*, 1978, **100**, 7472.
46. J. Wu, W. Liu, J. Ge, H. Zhang and P. Wang, *Chem. Soc. Rev.*, 2011, **40**, 3483.
47. J. B. Birks, Photophysics of Aromatic Molecules, Wiley, London, 1970.
48. T. S. Hsiao, S. L. Deng, K. Y. Shih and J. L. Hong, *J. Mater. Chem. C*, 2014, **2**, 4828.
49. T. Höfler and G. Wenz, *J. Inclus. Phenom. Mol.*, 1996, **25**, 81.
50. K. A. Udachin and J. A. Ripmeester, *J. Am. Chem. Soc.*, 1998, **120**, 1080.
51. M. T. Stone and H. L. Anderson, *Chem. Commun.*, 2007, 2387.
52. M. Okada, Y. Kawaguchi, H. Okumura, M. Kamachi and A. Harada, *J. Polym. Sci. Pol. Chem.*,2000, **38**, 4839.
53. J. Li, X. Ni, Z. Zhou and K. W. Leong, *J. Am. Chem. Soc.*, 2003, **125**, 1788.
54. M. V. Rekharsky and Y. Inoue, *Chem. Rev.*, 1998, **98**, 1875.
55. T. Ooya, H. S. Choi, A. Yamashita, N. Yui, Y. Sugaya, A. Kano, A. Maruyama, H. Akita, R. Ito, K. Kogure and H. Harashima, *J. Am. Chem. Soc.*, 2006, **128**, 3852.
56. X .Q. Guo, L. X. Song, F. Y. Du, Z. Dang and M. Wang, *J. Phys. Chem. B*, 2011, **115**, 1139.
57. L. X. Song, X. Q. Guo, F. Y. Du and L. Bai, *Polym. Degrad. Stabil.*,2010, **95**, 508.
58. Y. Liu, Y. L. Zhao, Y. Chen and M. Wang, *Macromol. Rapid Commun.*, 2005, **26**, 401.
59. M. E. Davis, *Mol. Pharmaceutics*, 2009, **6**, 659.
60. D. W. Pack1, A. S. Hoffman, S. Pun and P. S. Stayton, *Nat. Rev. Drug Discov.*, 2005, **4**, 581.
61. H. Okumura and Y. Kawaguchi and A. Harada, *Macromolecules*, 2001, **34**, 6338.
62. Y. Liu, A. Qin,X. Chen, X. Y. Shen, L. Tong, R. Hu, J. Z. Sun and B. Z. Tang, *Chem. Eur. J.*, 2011, **17**, 14736.
63. G. Liang, J. W. Y. Lam, W. Qin, J. Li, N. Xie and B. Z. Tang, *Chem. Commun.*, 2014, **50**, 1725.
64. S. Song, H. F. Zheng, D. M. Li, J. H. Wang, H. T. Feng, Z. H. Zhu, Y. C. Chen and Y. S. Zheng. *Org. Lett.*, 2014, **16**, 2170.
65. S. L Deng, P. C. Huang, L. Y. Lin, D. J. Yang and J. L. Hong *RSC Adv.*, 2015, **5**, 19512.
66. G. Fleury, G. Schlatter, C. Brochon and G, Hadziioannou, *Polymer*, 2005, **46**, 8494.
67. Z. Li, Y. Dong, B. Mi, Y. Tang, M. Häussler, H. Tong, Y. Dong, J. W. Y. Lam, Y. Ren, H. H. Y. Sung, K. S. Wong, P. Gao, I. D. Williams, H. S. Kwok and B. Z. J. Tang, *J. Phys. Chem. B*, 2005, **109**, 10061.
68. C. T. Lai, R. H. Chien, S. W. Kuo and J. L. Hong, *Macromolecules*, 2011, **44**, 6546.
69. X. Zhang, Z. Yang, Z. Chi, M. Chen, B. Xu, C. Wang, S. Liu, Y. Zhang, and J. Xu, *J. Mater. Chem.*, 2010, **20**, 292.
70. Y. Dong, J. W. Y. Lam, A. Qin, J. Sun, J. Liu, Z. Li, J. Sun, H. H. Y. Sung, I. D. Williams, H. S. Kwok and B. Z. Tang, *Chem. Commun.*, 2007, 3255.
71. H. Tong, Y. Dong, H. Häussler, J. W. Y. Lam, H. H. Y. Sung, I. D. Williams, J. Sun and B. Z. Tang, *Chem. Commun.*, 2006, 1133.
72. Y. Dong, J. W. Y. Lam, A. Qin, Z. Li, J. Sun, H. H. Y. Sung, I. D. Williams and B. Z. Tang, *Chem. Commun.*, 2007, 40.
73. H. Tong, Y. Dong, Y. Hong, H. Häussler, J. W. Y. Lam, H. H. Y. Sung, X. Yu, J. Sun, I. D. Williams, H. S. Kwok and B. Z. Tang, *Phys. Chem. C*, 2007, **111**, 2287.
74. L. Qian, B. Tong, J. Shen, J. Shi, J. Zhi, Y. Dong, F. Yang, Y. Dong, J. W. Y. Lam, Y. Liu and B. Z. J. Tang, *Phys. Chem. B*, 2009, **113**, 9098.